

3,4,5-Trimethoxychalcones Tubulin Inhibitors with a Stable Colchicine Binding Site as Potential Anticancer Agents

Maadh Jumaah¹, Tutik Dwi Wahyuningsih², and Melati Khairuddean^{1*}

¹School of Chemical Sciences, Universiti Sains Malaysia, 11800 Penang, Malaysia

²Department of Chemistry, Faculty of Mathematics and Natural Sciences, Universitas Gadjah Mada, Sekip Utara, Yogyakarta 55281, Indonesia

* **Corresponding author:**

tel: +604-6533560

email: melati@usm.my

Received: February 2, 2022

Accepted: April 23, 2022

DOI: 10.22146/ijc.72790

Abstract: The development of microtubule perturbing drugs is one of the most promising anticancer therapeutic methods. Unfortunately, limitation such as drug resistance, adverse side effects, complex formulations and synthesis, and limited bioavailability of these microtubule perturbing drugs has aroused the search for a new molecule of the tubulin system. Different substituents of chalcone were designed, synthesized, and determined for inhibition of tubulin assembly and toxicity in human cancer cell lines based on conventional colchicine site ligands and a computer model of the colchicine binding site on tubulin. A molecular docking study indicated that the chalcone scaffold could fit the colchicine site on tubulin in a similar orientation to the natural product. The 3,4,5-trimethoxyphenyl ring, which occupies the same sub-cavity as the equivalent molecule in colchicine, appeared to benefit the ligand of α,β -tubulin interaction. Several 3,4,5-trimethoxychalcone compounds demonstrated improved cytotoxicity against MCF-7 cells and inhibited tubulin assembly in vitro as potently as colchicine. The most active chalcone **1** with the IC_{50} of $6.18 \pm 0.69 \mu\text{M}$ prevented the proliferation of human cell lines at micromolar concentrations, causing microtubule destabilization and mitotic arrest in humans inhibiting breast cancer cells.

Keywords: microtubules; 3,4,5-trimethoxychalcone; docking study; colchicine; MCF-7 cells

■ INTRODUCTION

Microtubules (MTs) are cytoskeletal polymers made up of α,β -tubulin heterodimers that play a key role in cellular movement, division, and intracellular transport. Interfering with the assembly of MTs in dividing cells causes cell cycle arrest, resulting in apoptosis-inducing signals [1-2]. Therefore, the development of MT perturbing drugs is one of the most promising anticancer therapeutic methods [3-4]. Limitations, such as drug resistance, adverse side effects, complex formulations and synthesis, and limited bioavailability of these MT perturbing drugs [5] have continuously aroused the search for novel small molecules of the tubulin/MT system. MT-targeting drugs typically attach to one of the three primary tubulin binding sites which are taxane, vinca and colchicine sites [6] (Fig. 1). Taxanes and vinca

alkaloids have made significant contributions to the treatment of human cancers, but the toxicity of colchicine and podophyllotoxin has limited their therapeutic application in the treatment of cancer [7].

In this respect, the chemically versatile chalcones are an interesting scaffold for the discovery of new colchicine site ligands that inhibit tubulin assembly [8-10]. In the ongoing attempts to develop superior tubulin polymerization inhibitors, a series of chalcones **1-7** with aromatic substitution patterns resembling those found in conventional colchicine site ligands [11] (Fig. 1) have been synthesized. The molecular modeling was built to investigate the interactions of all the chalcones **1-7** with colchicine (PDB code: 1SA0). The docking experiments and prediction of pharmacokinetic properties and toxicity were carried out using the X-ray crystallographic

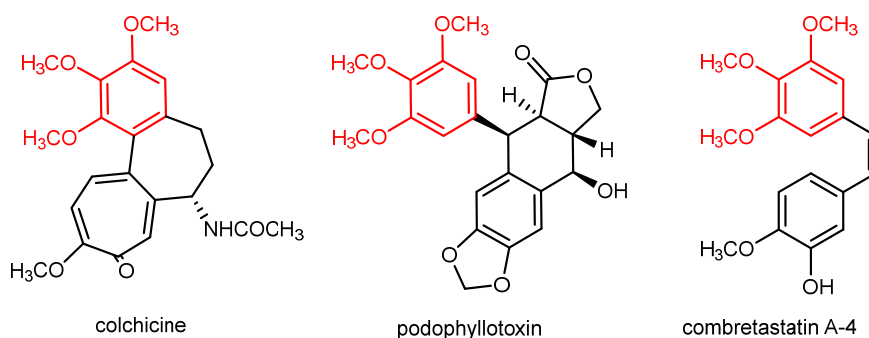


Fig 1. Microtubule-interacting agents that bind to tubulin's colchicine site

structure of colchicine in association with an inhibitor to investigate the binding affinity of these compounds at the active site.

■ EXPERIMENTAL SECTION

Materials

All the commercial chemicals and reagents in the syntheses were used without further purification; all chemicals, solvents, and materials used are as follows: QR&C, ASIA Sdn. Bhd.: acetic acid glacial, sulfuric acid (97%), hydrochloric acid (37%), acetone, chloroform, dichloromethane, diethyl ether, ethyl acetate, *n*-hexane, toluene, tetrahydrofuran, methanol (99.5%), ethanol (99.7%) and paraffin oil. Dimethyl sulfoxide-*d*₆ (Sigma-Aldrich, USA), sodium carbonate (99.99%, Merck, Germany), 3,4,5-trimethoxyacetophenone (97%, Sigma-Aldrich, Germany), 2-hydroxy-5-bromobenzaldehyde (98%, Sigma-Aldrich, China), 2-hydroxy-5-chlorobenzaldehyde (≥ 98%, Sigma-Aldrich, China), 2,5-dihydroxybenzaldehyde (≥ 98%, Sigma-Aldrich, China), 5-iodosalicylaldehyde (97%, Sigma-Aldrich, USA), 3-methoxy-2-hydroxybenzaldehyde (96%, Sigma-Aldrich, USA), 3-ethoxy-2-hydroxybenzaldehyde (96%, Sigma-Aldrich, USA); TLC silica gel 60 F254, aluminum sheet, 20 cm × 20 cm (Merck, Germany) and silica gel 60 (70–230 mesh).

Instrumentation

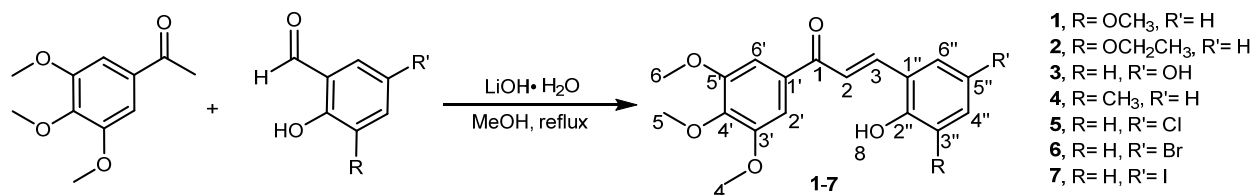
Instruments used included Thin-layer chromatography (TLC) uses a commercially available aluminum-supported silica gel 60F₂₅₄ plate, which was observed under CAMAG® Ultra Violet (UV) lamp (254 and 386 nm). The melting points were determined using the

Stuart Scientific SMP1 equipment in the temperature range of 25–350 °C. The functional groups of the compounds were determined using the FTIR Perkin Elmer 2000 spectrometer. The ¹H and ¹³C-NMR spectra were obtained using a 500 MHz Bruker Avance spectrometer. The CHN elemental analysis is used to determine the amount of carbon (C), hydrogen (H), and nitrogen (N) in a sample using a Perkin Elmer II, 2400 CHN analyzer.

Procedure

A mixture of 3,4,5-trimethoxyacetophenone (0.3 g) in MeOH (20 mL), LiOH·H₂O (0.5 g), and disubstituted benzaldehyde (0.12 g) was refluxed and the reaction progress was monitored by TLC (Scheme 1). After quenching the reaction with dilute hydrochloric acid, the solution was extracted with ethyl acetate. The organic layer was washed with aqueous NaHCO₃, water, and brine before it was dried over anhydrous Na₂SO₄. The crude was concentrated and purified using column chromatography with *n*-hexane/ethyl acetate (10:1) as an eluent.

(E)-3-(2-hydroxy-3-methoxyphenyl)-1-(3,4,5-trimethoxyphenyl)prop-2-en-1-one, 1. Yield: 84.8%, pine-green powder; m.p: 168–171 °C. IR (cm⁻¹): 3336 (-OH); 2946, 2839 (C-H sp³); 1620 (C=O); 1611 and 1583 (C=C). ¹H-NMR (500 MHz, DMSO-*d*₆) δ, ppm: 8.05 (d, *J* = 15.7 Hz, 1H, H-3); 7.84 (d, *J* = 15.7 Hz, 1H, H-2); 7.45 (d, *J* = 2.7, 1H, H-3''); 7.40 (s, 2H, H-6', H-2'); 6.93 (dd, *J*₁ = 2.7 Hz, *J*₂ = 8.9 Hz, 1H, H-4''); 6.91 (d, *J* = 8.9 Hz, 1H, H-6''); 6.15 (s, 1H, H-8); 3.90 (s, 6H, H-4,6); 3.77 (s, 3H, H-5); 3.76 (s, 3H, H-7). ¹³C-NMR (125 MHz, DMSO-*d*₆) δ, ppm: 188.7 (C-1); 153.4 (C-5', C-3'); 152.7 (C-2''); 142.3 (C-4'); 139.7 (C-1'); 133.8 (C-3); 130.1 (C-5''); 122.2 (C-3'');



Scheme 1. Synthesis of chalcones 1-7

121.4 (C-2); 119.1 (C-1''); 117.6 (C-4''); 112.8 (C-6''); 106.6 (C-6', C-2''); 60.7 (C-5); 56.7 (C-4, C-6); 56.1 (C-7). CHN Elemental analysis: Calculated for C₁₉H₂₀O₆: C, 66.27; H, 5.85. Found: C, 65.97; H, 5.57.

(E)-3-(3-ethoxy-2-hydroxyphenyl)-1-(3,4,5-trimethoxyphenyl)prop-2-en-1-one, 2. Yield: 65.8%, brown powder; m.p: 177–179 °C. IR (cm⁻¹): 3336 (-OH); 2946, 2839 (C-H sp³); 1620 (C=O); 1611 and 1583 (C=C). ¹H-NMR (500 MHz, DMSO-*d*₆) δ, ppm: 8.15 (d, *J* = 15.7 Hz, 1H, H-3); 7.81 (d, *J* = 15.7 Hz, 1H, H-2); 7.55 (d, *J* = 2.7, 1H, H-3''); 7.33 (s, 2H, H-6', H-2''); 6.93 (dd, *J*₁ = 2.7 Hz, *J*₂ = 8.9 Hz, 1H, H-4''); 6.91 (d, *J* = 8.9 Hz, 1H, H-6''); 6.15 (s, 1H, H-8); 3.90 (s, 6H, H-4,6); 3.77 (s, 3H, H-5); 3.76 (s, 3H, H-7). ¹³C-NMR (125 MHz, DMSO-*d*₆) δ, ppm: 189.7 (C-1); 154.4 (C-5', C-3'); 151.7 (C-2''); 142.3 (C-4'); 141.1 (C-1''); 133.8 (C-3); 130.1 (C-5''); 122.2 (C-3''); 121.4 (C-2); 120.0 (C-1''); 118.6 (C-4'') 112.7 (C-6''); 108.2 (C-6', C-2''); 60.9 (C-5); 56.7 (C-4, C-6); 56.1 (C-7). CHN Elemental analysis: Calculated for C₁₉H₂₀O₆: C, 66.27; H, 5.84. Found: C, 65.98; H, 5.56.

(E)-3-(2,3-dihydroxyphenyl)-1-(3,4,5-trimethoxyphenyl)prop-2-en-1-one, 3. Yield: 78.4%, yellow powder; m.p: 195–198 °C. IR (cm⁻¹): 3238 (-OH), 2935, 2839 (C-H sp³), 1648 (C=O), 1589 and 1552 (C=C). ¹H-NMR (500 MHz, 1,2-dichloroethane-*d*₄) δ, ppm: 11.03 (s, 1H), 8.33 (d, *J* = 16.2 Hz, 1H), 8.23 (d, *J* = 8.9 Hz, 1H), 7.60 (d, *J* = 16.2 Hz, 1H), 7.25 (d, *J* = 7.7 Hz, 2H), 7.10 (s, 2H), 4.64 (s, 3H), 4.54 (s, 3H), 4.50 (s, 6H). ¹³C-NMR (125 MHz, 1,2-dichloroethane-*d*₄) δ, ppm: 195.0, 163.7, 162.9, 159.5, 159.2, 141.1, 131.1, 127.3, 115.6, 112.8, 107.6, 102.3, 92.3, 57.0, 56.7, 56.4. CHN Elemental analysis: Calculated for C₁₉H₂₀O₆: C, 66.27; H, 5.85. Found: C, 65.99; H, 5.56.

(E)-3-(2-hydroxy-3-methylphenyl)-1-(3,4,5-trimethoxyphenyl)prop-2-en-1-one, 4. Yield: 72.5%, golden-yellow powder; m.p: 142–145 °C. IR (cm⁻¹): 3176 (-OH); 2943, 2836 (C-H sp³); 1636 (C=O); 1586 and 1558

(C=C). ¹H-NMR (500 MHz, DMSO-*d*₆) δ, ppm: 10.01 (s, 1H, H-8); 8.07 (d, *J* = 15.5 Hz, 1H, H-3); 7.81 (d, *J* = 15.5 Hz, 1H, H-2); 7.70 (s, 1H, H-3''); 7.30 (s, 2H, H-6', H-2''); 7.08 (dd, *J*₁ = 1.8 Hz, *J*₂ = 8.3 Hz, 1H, H-4''); 6.85 (d, *J* = 8.3 Hz, 1H, H-6''); 3.90 (s, 6H, H-4,6); 3.77 (s, 3H, H-5); 2.27 (s, 3H, H-7). ¹³C-NMR (125 MHz, DMSO-*d*₆) δ, ppm: 188.5 (C-1); 155.6 (C-2''); 153.4 (C-5', C-3'); 142.3 (C-4'); 139.8 (C-1'); 133.8 (C-3); 133.3 (C-5''); 128.8 (C-3''); 128.4 (C-1''); 121.6 (C-2); 120.8 (C-4''); 116.6 (C-6''); 106.6 (C-6', C-2''); 60.7 (C-5); 56.7 (C-4, C-6); 20.6 (C-7). CHN Elemental analysis: Calculated for C₁₉H₂₀O₅: C, 66.27; H, 5.85. Found: C, 66.01; H, 5.56.

(E)-3-(5-chloro-2-hydroxyphenyl)-1-(3,4,5-trimethoxyphenyl)prop-2-en-1-one, 5. Yield: 62.4%, yellow powder; m.p: 221–225 °C. IR (cm⁻¹): 3207 (-OH), 2937, 2839 (C-H sp³), 1603 (C=O), 1583 and 1508 (C=C). ¹H-NMR (500 MHz, DMSO-*d*₆) δ, ppm: 10.44 (s, 1H), 7.68 (d, *J* = 2.1 Hz, 1H), 7.42 (d, *J* = 16.5 Hz, 1H), 7.25 (dd, *J*₁ = 2.2 Hz, *J*₂ = 8.7 Hz, 1H), 7.00 (d, *J* = 16.5 Hz, 1H), 6.90 (d, *J* = 8.7 Hz, 1H), 6.30 (s, 2H), 3.83 (s, 3H), 3.71 (s, 6H). ¹³C-NMR (125 MHz, DMSO-*d*₆) δ, ppm: 193.1, 162.4, 158.5, 155.9, 138.1, 131.6, 129.3, 128.0, 123.7, 123.3, 118.3, 111.6, 91.6, 56.3, 55.9. CHN Elemental analysis: Calculated for C₁₈H₁₇ClO₅: C, 61.99; H, 4.96. Found: C, 61.69; H, 4.67.

(E)-3-(5-bromo-2-hydroxyphenyl)-1-(3,4,5-trimethoxyphenyl)prop-2-en-1-one, 6. Yield: 67.9%, yellow powder; m.p: 171–174 °C. IR (cm⁻¹): 3154 (-OH); 2949, 2833 (C-H sp³); 1645 (C=O); 1566 and 1507 (C=C). ¹H-NMR (500 MHz, DMSO-*d*₆) δ, ppm: 9.61 (s, 1H, H-8); 8.12 (d, *J* = 2.3 Hz, 1H, H-3''); 7.96 (d, *J* = 15.5 Hz, 1H, H-3); 7.94 (d, *J* = 15.5 Hz, 1H, H-2); 7.42 (s, 2H, H-6', H-2''); 7.40 (dd, *J*₁ = 2.4 Hz, *J*₂ = 8.7 Hz, 1H, H-4''); 6.98 (d, *J* = 8.7 Hz, 1H, H-6''); 3.90 (s, 6H, H-4,6); 3.77 (s, 3H, H-5). ¹³C-NMR (125 MHz, DMSO-*d*₆) δ, ppm: 188.5 (C-1); 156.8 (C-2''); 153.4 (C-5', C-3'); 142.5 (C-

4'); 137.8 (C-1'); 134.7 (C-5''); 133.5 (C-3); 130.7 (C-3''); 124.2 (C-1''); 122.3 (C-2); 118.8 (C-4''); 111.3 (C-6''); 106.8 (C-6', C-2'); 60.7 (C-5); 56.8 (C-4,C-6). CHN Elemental analysis: Calculated for C₁₈H₁₇BrO₅: C, 54.98; H, 4.36. Found: C, 54.68; H, 4.06.

(E)-3-(2-hydroxy-5-iodophenyl)-1-(3,4,5-trimethoxyphenyl)prop-2-en-1-one, 7. Yield: 88.4%, brown powder; m.p: 197–200 °C. IR (cm⁻¹): 3218 (-OH), 2929, 2845 (C-H sp³), 1600 (C=O), 1583 and 1500 (C=C). ¹H-NMR (500 MHz, DMSO-*d*₆) δ, ppm: 10.43 (s, 1H, H-8), 7.89 (d, *J* = 1.9 Hz, 1H, H-3''), 7.51 (dd, *J*₁ = 2.0 Hz, *J*₂ = 8.6 Hz, 1H, H-4''), 7.37 (d, *J* = 16.3 Hz, 1H, H-3), 7.00 (d, *J* = 16.3 Hz, 1H, H-2), 6.73 (d, *J* = 8.6 Hz, 1H, H-6''), 6.30 (s, 2H, H-6', H-2'), 3.83 (s, 3H, H-5), 3.71 (s, 6H, H-4,6). ¹³C-NMR (125 MHz, DMSO-*d*₆) δ, ppm: 194.0 (C-1); 162.4 (C-2''); 158.5 (C-5', C-3''); 156.9 (C-4''); 140.2 (C-1'); 138.1 (C-5''); 136.9 (C-3); 129.9 (C-3''); 124.5 (C-1''); 119.2 (C-2); 111.7 (C-4''); 91.5 (C-6''); 82.1 (C-6', C-2'); 56.3 (C-5); 55.9 (C-4,6). CHN Elemental analysis: Calculated for C₁₈H₁₇IO₅: C, 49.11; H, 3.89. Found: C, 48.82; H, 3.58.

Cytotoxicity assay

Cell culture. The MCF-7 cell for human breast cancer was obtained from the American Type Culture Collection (ATCC, USA) in addition to 10% (v/v) of the Fetal Bovine Serum (FBS) from the Rosewell Park Memorial Institute 1640 (RPMI), (GE Healthcare HyClone, Kansas, USA). The cells were kept at 37 °C in an incubator (Memmert, Germany) with 5% CO₂ and 95% humidity. The cells were divided every two to three days or when they reached 80–90% confluency on the culture flask surface. The spent media were removed to eliminate any leftover serum that may inactivate trypsin activity and cells were washed with 1 to PBS (MediaTech, United States). Following the removal of the PBS, 2 mL of trypsin solution (SAFC Biosciences, USA) was added to the flask. Cells were incubated at 37 °C for 10 min to enable them to detach from the surface of the culture flask (Nunc, Denmark). Then, 6 mL of appropriate growth medium was added to inactivate the trypsin activity in the ratio of 1:3 (1 = trypsin; 3 = growth medium) to a Falcon tube of 15 mL. After trypsinizing the cells, they were centrifuged at 1500 rpm for 5 min, and the supernatant was discarded. The cell pellet was re-suspended in 8 mL of new growth

medium before being divided into the prepared culture flasks for further usage.

Cell counting. A dye exclusion viability test in a hemocytometer was used to measure the number of cells in a particular population. The cell monolayers were unbundled by trypsinization, centrifugation, and medium re-suspension. The cell suspension (20 mL) was combined with 20 mL of a 0.08% (v/v) trypan blue dye solution (Merck, Germany) to produce a trypan blue dye solution. A capillary action distributed the solution uniformly across the counting chamber of a hemocytometer after it had been put there. The average number of viable cells in each of the four-square grid corners was determined by looking through an inverted fluorescence microscope (Nikon, Japan) at 100× magnification to count the number of unstained viable cells in each of the four-square grid corners. Each square grid represents a 0.0001 mL volume, and the cell concentration was calculated using Eq. (1) and a dilution factor of two. To measure the percentage of cell viability, both dead (stained) and viable (unstained) cells were counted individually, and the results were computed as shown in Eq. (2). Between samples and after usage, the hemocytometer slide and glass coverslip were promptly washed and cleaned with 70% (v/v) ethanol (Thermo Scientific, USA) to remove any remaining residue.

$$C = (n/v) \times D \quad (1)$$

$$\% \text{ Viability} = (Nv/Nv + ND) \times 100\% \quad (2)$$

where C: cell concentration (cells/mL), N: average number of cells, v: volume counted (mL), D: dilution factor, Nv: total number of visible cells, and ND: total number of dead cells.

MTT assay

The cytotoxicity of the compounds was determined using the MTT cell viability test. The MCF-7 cell lines were plated at a density of about 2×10^4 cells/well in a 96-well plate and incubated overnight before being treated with chalcone analogs at different doses (0–100 g) and incubated for another 24 h. Following incubation, 20 μL of MTT reagent (5 g/L) was applied to each well of the microplate, followed by 90 min in the dark at 37 °C. The spent medium was discarded, and the purple formazan precipitates were

dissolved in 200 μ L of dimethyl sulfoxide (DMSO). To detect the absorbance of the solution, the optical density was measured using a microplate reader (Tecan Sunrise, Switzerland) at a test wavelength of 570 nm and a reference wavelength of 650 nm. The test was carried out in triplicate to determine the percentages of viable cells in comparison to the DMSO control. The half-maximal inhibitory concentration (IC_{50}) value was calculated from the data using the dose-response curve fitting graph at 50% cell viability.

Cytotoxic effect of the synthesized compounds on MCF-7 cells. The cell-based assays count the number of viable cells on multi-well plates and determine if a chemical affects cell growth or has direct cytotoxic effects that result in cell death. Regardless of the kind of cell-based assay employed, it is critical to know the number of viable cells left in an experiment. The antiproliferative activity was measured using 3-(4,5-dimethylthiazol-2-yl)-2,5-diphenyltetrazolium bromide (MTT) reduction assay, which is the most widely used assay and was the first homogeneous cell viability assay developed for a 96-well plate, making it suitable for high throughput screening. The viable cells with active metabolism convert the yellow tetrazolium MTT into the insoluble (*E,Z*)-5-(4,5-dimethylthiazol-2-yl)-1,3-diphenylformazan (formazan), a purple crystal. A dying cell lost the ability to convert MTT to formazan. When formazan is produced, it is dissolved in DMSO to give a purple solution with a distinctive absorbance at 540 nm. The intensity of the purple color is related to the cell count, showing the vitality of the cells. The antitumor efficacy of all chalcone-based drugs was determined *in vitro* against breast cancer cell lines (MCF-7) using a previously described MTT test. The IC_{50} values, which are employed as a cytotoxicity measure, relate to the proportion of cells inhibited by 3,4,5-trimethoxychalcone compounds. The inhibitory activity of drugs was determined after a 24-h exposure and was represented as the concentration needed to decrease tumor cell growth by 50% (IC_{50}). All results are expressed as means standard deviations of three separate experiments. The antiproliferative effect of paclitaxel was also evaluated using the MCF-7 cell line as a positive control.

Molecular modeling

α,β -Tubulin was chosen as the target receptor and was obtained from the Protein Data Bank. α,β -Tubulin-colchicine complex site inhibitors were developed using a structure-based approach with the reported protein crystal structure of colchicine obtained from the Protein Data Bank (<http://www.rcsb.org/>, PDB code: 1SA0). The potential inhibitors, trimethoxy and *ortho*-hydroxy chalcone, were designed based on the common similarities shared with those reported colchicine inhibitors by molecular docking, which was chosen based on the binding energy and inhibition constant of the chalcones. The ligand structures were drawn using Marvin-Sketch and BIOVIA to observe the ligand-protein interactions. Structure files were prepared for molecular docking by defining the number of torsion angles and hydrogen atoms. To validate the feasibility of the Autodock Vina with Chimera 1.12 programs, the docking studies were first performed on the reference compounds colchicine to predict the binding mode of the design compounds, and the calculations of AutoDock Vina were performed on a Windows Intel® Pentium® Core (TM) i5-2450M Quad CPU 4.00 GHz operating system. All structure images above were displayed using PyMOL viewer.

■ RESULTS AND DISCUSSION

Chemistry

The preparation of chalcones 1-7, as shown in Scheme 1, was easily obtained in good yield via a Claisen-Schmidt condensation of an aromatic aldehyde with an aliphatic ketone using LiOH•H₂O as a catalyst in refluxing methanol. Purification using column chromatography with *n*-hexane/ethyl acetate (10:1) as an eluent gave the expected compounds, which were characterized using ¹H-NMR spectroscopy and IR spectrometry.

Antiproliferative Properties of Chalcone Compounds against Breast Cancer Cell Line (MCF-7)

Chalcones 1-7, as small molecule inhibitors, were tested on MCF-7 human breast cancer cell lines.

Paclitaxel was used as a reference drug against MCF-7 in the MTT experiment. The inhibitory activity was measured after 24-h exposure to chemicals and expressed as the IC₅₀ value. All data are presented as the means and standard deviations \pm SDs of three independent experiments. Upon investigation of the inhibitory effects of substances, paclitaxel was also used as a positive control for the MCF-7 cell line to examine its antiproliferative efficacy.

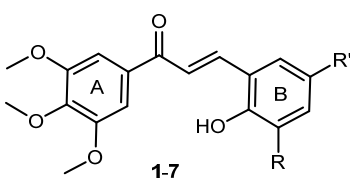
As shown in Table 1, chalcone **1** has the most potent activity with the IC₅₀ of $6.18 \pm 0.69 \mu\text{M}$, compared to other chalcones, and was even more potent than the positive control, paclitaxel (IC₅₀: $15 \mu\text{M}$). However, compounds **3**, **4**, and **5** showed moderate activity below $50 \mu\text{M}$. Since the rest of the samples showed poor cytotoxicity, the IC₅₀ values for such compounds could not be determined. The chemical structure and biological activity correlated through structure-activity relationship (SAR) analysis deduced that the trimethoxy substituents in ring A and the planar structure of fully aromatized *ortho*-hydroxy chalcones with another different substituent in ring B formed interesting cytotoxicity activities. Studies have demonstrated that the *ortho*-hydroxy chalcone or trimethoxy groups can intercalate into DNA and inhibit tubulin polymerization [12-14]. Consistent with molecular modeling expectations, chalcones inhibited MCF-7 proliferation and tubulin assembly more

effectively than the positive control paclitaxel, which retained growth inhibitory activity against MCF-7 cells. In this study, the influence of the substituents on the aromatic ring attached to the *ortho*-hydroxy position of the chalcone ring (B) system on the cytotoxic potency has also been investigated. Compounds with *ortho*-hydroxy chalcones with a variety of substituents at positions-3 and -5 have been reported to inhibit MCF-7, as shown in Table 1. Interestingly, these chalcone-based compounds possess diverse structural properties with various substituents, most of which are electron-donating functionalities, such as methoxy functional groups, at different positions of both aromatic systems. It was observed that 3-methoxy substituent displayed MCF-7 inhibition more than 3-ethoxy and 3-CH₃. The position of the substituent on the aromatic ring (*meta*, *para*, or *ortho*) has also influenced the cytotoxic activity. From data collected in Table 1, the SARs study has also revealed that compounds with another substituent, such as Cl, Br, and I, showed that the replacement of bromo substituent at position 5 to chloro has also influenced the cytotoxic activity from 60 to $46.36 \mu\text{M}$ against MCF-7.

Structure-Based Drug Design

To gain a better understanding of the efficacy of the synthesized compounds, their interactions with the

Table 1. Antiproliferative activities of chalcones **1-7** and docking parameters



1, R= OCH₃, R'= H
 2, R= OCH₂CH₃, R'= H
 3, R= H, R'= OH
 4, R= CH₃, R'= H
 5, R= H, R'= Cl
 6, R= H, R'= Br
 7, R= H, R'= I

Compound	M.W. (g/mol)	Log p	H-bond donor	H-bond acceptor	Free binding energy (kcal/mol)	IC ₅₀ MCF-7 (μM) ^a
1	344.36	2.62	1	6	-9.4	6.18 ± 0.69
2	358.39	2.97	1	6	-8.7	> 50
3	360.41	2.60	2	6	-8.6	38.48 ± 0.64
4	328.36	3.32	2	5	-8.4	48.62 ± 0.69
5	348.78	3.40	1	5	-8.1	46.36 ± 0.90
6	393.23	3.64	2	5	-7.5	> 60
7	440.23	3.87	1	5	-7.7	> 100
Paclitaxel	853.91	3.30	4	10	-8.9	15

^a The data are presented as the mean \pm SE from at least two separate dose-response curves

tubulin crystal structure were examined. The classical ligand of the colchicine site on tubulin (Fig. 1) contains 3,4,5-trimethoxyphenyl groups [15-17], which is linked to increased antiproliferative potency in potential inhibitors. The trimethoxy chalcones 1-7 were designed based on the common similarities of the reported colchicine inhibitors [18], with the conditions consistent with those described in a series of potent colchicine. For a molecule to have drug-like properties which might be pharmacologically active in humans, these compounds need to meet Lipinski's rule of five, which specifies that the number of hydrogen bond donors (5), hydrogen bond acceptors (10), molecular weight less than 500 g/mol and octanol-water partition coefficient log P less than 5 [19]. To evaluate the properties of a compound which might be pharmacological active in humans, the prediction of ADME properties was performed. Herein, the drug-likeness, solubility, and drug score values for chalcones 1-7 were determined to analyze their overall potential and to confirm whether they are qualified to become promising drugs. These were compared with drugs that are currently used against MCF-7, such as paclitaxel and colchicine. The drug-likeness value is calculated based on the occurrence frequency of the analyzed molecules compared to the commercial drugs and non-drug-like compounds. Potential toxicity, solubility, and drug-like properties (drug score) of the chalcones 1-7 were estimated by Osiris Property Explorer. According to the Osiris database, more than 80% of the traded drugs have predicted solubility values; as shown in Table 2, the

synthesized chalcones 1-7 exhibited solubility values between -3.30 and -4.61.

In the Osiris program, the occurrence frequency of each fragment is determined within the collection created by shredding 3300 traded drugs as well as 15,000 commercially available chemicals (Fluka), yielding a complete list of all available fragments. In this case, positive values point out that the molecule contains predominantly better fragments, which are frequently present in commercial drugs but not in the non-druglike collection of Fluka compounds. The drug score combines drug-likeness and toxicity risks in one value that may be used to judge the drug potential of a compound. Interestingly, chalcones (1, 5, and 7) have positive drug-likeness (5.35-7.16) and drug score (0.38-0.71) values were similar to or even better than some of the drugs currently used in the market (Table 2). The drug score unites properties such as drug-likeness, solubility, and toxicity risks in one parameter that may be used to estimate the compound's potential to qualify as a drug.

Positive Control Docking

All chalcones 1-7 were docked into the binding pocket of the target protein to determine the ligand's potential poses. The root mean square deviation (RMSD) in a molecular docking study refers to the ability of docking programs to replicate the ligand binding mode to match the target protein crystal structure [20]. The docking techniques are validated only

Table 2. Estimation of toxicity, solubility, drug-likeness, and drug score for chalcones 1-7

Compound	Toxicity risks ^{a)}				Solubility	Drug-likeness	Drug score
	Mutagenicity	Tumorigenicity	Irritation	Reproductive			
1	-	-	-	-	-3.62	5.35	0.38
2	++	-	+	-	-3.92	3.90	0.75
3	-	-	+	-	-3.30	5.17	0.84
4	-	-	++	-	-3.94	5.28	0.46
5	-	-	-	-	-4.33	7.13	0.71
6	-	-	-	-	-4.43	5.00	0.66
7	-	-	-	-	-4.61	7.16	0.62
Colchicine	-	-	-	++	-3.05	1.02	0.42
Paclitaxel	-	-	-	-	-6.29	0.19	0.22

^{a)} -: low risk; +: moderate risk; ++: high risk

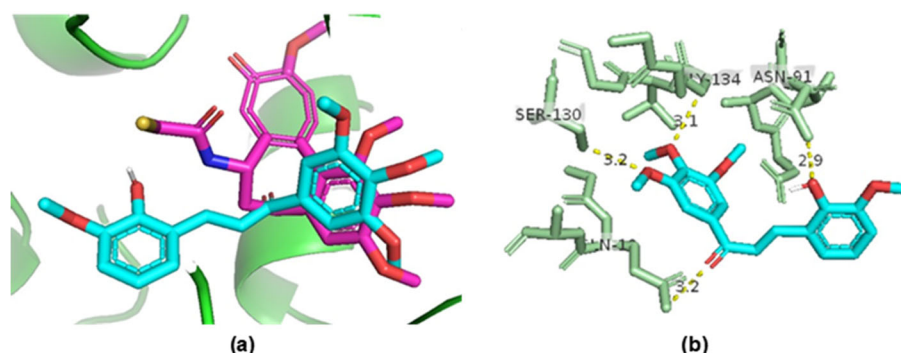


Fig 2. (a) Overview of the binding mode of chalcone **1** in the tubulin crystal structure, (b) close view of the potential binding pose of chalcone **1** in colchicine (PDB code: 1SA0)

when re-docked ligands exhibit the same docking pose as the reported protein-ligand complex, which is referred to as positive control docking. A lower RMSD value of less than 2.0 Å means higher docking accuracy, which indicates successful docking [21]. In this study, the target protein used was colchicine crystal structure (PDB code: 1SA0). Chalcone was re-docked on the active location of the same complex of colchicine and resulted in the RMSD value of 0.42. The data obtained verified that the docking experiments were highly accurate for the possible chalcone inhibitors.

In molecular docking experiments, chalcones **1-7** showed good free binding energy for the protein-ligand interaction in the range of -7.3 to -9.4 kcal/mol (Table 1). The binding energy is comparable with the interaction of the positive control, paclitaxel, and colchicine in the active site of the protein. Molecular docking of chalcone **1** exhibited the best anti-proliferative activity and was chosen as the optimum compound for further investigation. The amino acid residue which had interaction with tubulin was labeled. In the binding mode, compound **1** was nicely bound to the colchicine binding site of tubulin via hydrophobic interaction and binding was stabilized by a hydrogen bond. The calculated binding energies were used as the parameters for the selection of the cluster of docking posed to be evaluated, in which the binding mode of the lowest energy structure is located in the top docking cluster. The selected pose of chalcone **1** showed the interactions of methoxy oxygen (O-GLY-134; 3.1), methoxy oxygen (O-SER-130; 3.2),

carbonyl oxygen (O-GLN-10; 3.2), and hydroxy (O-ASN-91; 2.9), as observed in Fig. 2. This molecular docking result, along with the biological test results, suggests that chalcone **1** may be a tubulin inhibitor.

■ CONCLUSION

A new series of 3,4,5-trimethoxychalcone **1-7** were successfully synthesized and characterized. Evaluation of their cytotoxic and tubulin polymerization inhibitor activity showed significant anticancer properties, which are comparable with that of the reference drug, paclitaxel. Among these compounds, chalcone **1** exhibits the best free binding energy of -9.4 kcal/mol, which is comparable with the interaction of the positive control, paclitaxel, and colchicine in the active site of the protein. Chalcone **1** showed the most potent MCF-7 inhibitory activity ($IC_{50} = 6.18 \pm 0.69 \mu\text{M}$), which is a potential tubulin polymerization inhibitor. The binding of chalcone **1** with colchicine showed one protein-ligand interaction and hydrophobic interactions with the protein residues in the ASN-2 binding site, which might play essential roles in its colchicine inhibition and antiproliferative activity. Chalcones (**1**, **5**, and **7**) have been shown water solubility, ADME properties, and toxicity profile were similar to or even better than some of the drugs currently used in the market, such as paclitaxel. Thus, in search of inhibitors with potent activity, chalcone **1**, as well as other chalcone derivatives containing 3,4,5-trimethoxy and hydroxy groups, are promising compounds as potential anticancer agents.

■ ACKNOWLEDGMENTS

The authors would like to thank the Ministry of Higher Education Malaysia for the Fundamental Research Grant Scheme with project code FRGS/1/2019/STG01/USM/02/16, which was used to finance this research work.

■ REFERENCES

- [1] Ilan, Y., 2019, Microtubules: From understanding their dynamics to using them as potential therapeutic target, *J. Cell. Physiol.*, 234 (6), 7923–7937.
- [2] Downing, K.H., and Nogales, E., 1998, Tubulin structure: Insights into microtubule properties and functions, *Curr. Opin. Struct. Biol.*, 8 (6), 785–791.
- [3] Dumontet, C., and Jordan, M.A., 2010, Microtubule-binding agents: A dynamic field of cancer therapeutics, *Nat. Rev. Drug Discovery*, 9 (10), 790–803.
- [4] Arnst, K.E., Banerjee, S., Chen, H., Deng, S., Hwang, D.J., Li, W., and Miller, D.D., 2019, Current advances of tubulin inhibitors as dual-acting small molecules for cancer therapy, *Med. Res. Rev.*, 39 (4), 1398–1426.
- [5] Čermák, V., Dostál, V., Jelínek, M., Libusová, L., Kovář, J., Rösel, D., and Brábek, J., 2020, Microtubule-targeting agents and their impact on cancer treatment, *Eur. J. Cell Biol.*, 99 (4), 151075.
- [6] Steinmetz, M.O., and Prota, A.E., 2018, Microtubule-targeting agents: Strategies to hijack the cytoskeleton, *Trends Cell Biol.*, 28 (10), 776–792.
- [7] Karahalil, B., Yardım-Akaydin, S., and Nacak Baytas, S., 2019, An overview of microtubule targeting agents for cancer therapy, *Arh. Hig. Rada Toksikol.*, 70 (3), 160–172.
- [8] Dyrager, C., Wickström, M., Fridén-Saxin, M., Friberg, A., Dahlén, K., Wallén, E.A.A., Gullbo, J., Gröthli, M., and Luthman, K., 2011, Inhibitors and promoters of tubulin polymerization: Synthesis and biological evaluation of chalcones and related dienones as potential anticancer agents, *Bioorg. Med. Chem.*, 19 (8), 2659–2665.
- [9] Ouyang, Y., Li, J., Chen, X., Fu, X., Sun, S., and Wu, Q., 2021, Chalcone derivatives: Role in anticancer therapy, *Biomolecules*, 11 (6), 894.
- [10] Liu, W., He, M., Li, Y., Peng, Z., and Wang, G., 2022, A review on synthetic chalcone derivatives as tubulin polymerisation inhibitors, *J. Enzyme Inhib. Med. Chem.*, 37 (1), 9–38.
- [11] Jumaah, M., Khairuddean, M., Owaid, S.J., Zakaria, N., Mohd Arshad, N., Nagoor, N.H., and Mohamad Taib, M.N.A., 2022, Design, synthesis, characterization and cytotoxic activity of new *ortho*-hydroxy and indole-chalcone derivatives against breast cancer cells (MCF-7), *Med. Chem. Res.*, 31 (3), 517–532.
- [12] Peng, F., Meng, C.W., Zhou, Q.M., Chen, J.P., and Xiong, L., 2016, Cytotoxic evaluation against breast cancer cells of isoliquiritigenin analogues from *Spatholobus suberectus* and their synthetic derivatives, *J. Nat. Prod.*, 79 (1), 248–251.
- [13] Karthikeyan, C., Narayana Moorthy, N.S.H., Ramasamy, S., Vanam, U., Manivannan, E., Karunakaran, D., and Trivedi, P., 2015, Advances in chalcones with anticancer activities, *Recent Pat. Anti-Cancer Drug Discovery*, 10 (1), 97–115.
- [14] Shin, S.Y., Kim, J.H., Yoon, H., Choi, Y.K., Koh, D., Lim, Y., and Lee, Y.H., 2013, Novel antimitotic activity of 2-hydroxy-4-methoxy-2',3'-benzochalcone (HymnPro) through the inhibition of tubulin polymerization, *J. Agric. Food Chem.*, 61 (51), 12588–12597.
- [15] McLoughlin, E.C., and O'Boyle, N.M., 2020, Colchicine-binding site inhibitors from chemistry to clinic: A review, *Pharmaceuticals*, 13 (1), 8.
- [16] Kumbhar, B.V., Borogaon, A., Panda, D., and Kunwar, A., 2016, Exploring the origin of differential binding affinities of human tubulin isoforms α II, α III and α IV for DAMA-colchicine using homology modelling, molecular docking and molecular dynamics simulations, *PLoS One*, 11 (5), e0156048.
- [17] Salum, L.B., Mascarello, A., Canevarolo, R.R., Altei, W.F., Laranjeira, A.B., Neuenfeldt, P.D., Stumpf, T.R., Chiaradia-Delatorre, L.D., Vollmer, L.L., Daghestani, H.N., de Souza Melo, C.P., Silveira, A.B., Leal, P.C., Frederico, M.J.S., do Nascimento, L.F., Santos, A.R.S., Andricopulo, A.D., Day, B.W., Yunes,

- R.A., Vogt, A., Yunes, J.A., and Nunes, R.J., 2015, *N*-(1'-naphthyl)-3,4,5-trimethoxybenzohydrazide as microtubule destabilizer: Synthesis, cytotoxicity, inhibition of cell migration and in vivo activity against acute lymphoblastic leukemia, *Eur. J. Med. Chem.*, 96, 504–518.
- [18] Dong, M., Liu, F., Zhou, H., Zhai, S., and Yan, B., 2016, Novel natural product-and privileged scaffold-based tubulin inhibitors targeting the colchicine binding site, *Molecules*, 21 (10), 1375.
- [19] Lipinski, C.A., Lombardo, F., Dominy, B.W., and Feeney, P.J., 2001, Experimental and computational approaches to estimate solubility and permeability in drug discovery and development settings, *Adv. Drug Delivery Rev.*, 46 (1-3), 3–26.
- [20] Ramírez, D., and Caballero, J., 2018, Is it reliable to take the molecular docking top scoring position as the best solution without considering available structural data?, *Molecules*, 23 (5), 1038.
- [21] Torres, P.H.M., Sodero, A.C.R., Jofily, P., and Silva-Jr, F.P., 2019, Key topics in molecular docking for drug design, *Int. J. Mol. Sci.*, 20 (18), 4574.